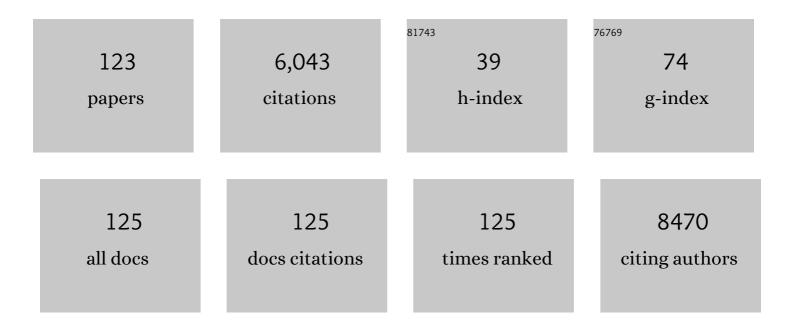
List of Publications by Year in descending order

Source: https://exaly.com/author-pdf/8051215/publications.pdf Version: 2024-02-01



LIE ZHENC

#	Article	IF	CITATIONS
1	Rational design of a metal–organic framework host for sulfur storage in fast, long-cycle Li–S batteries. Energy and Environmental Science, 2014, 7, 2715.	15.6	434
2	Directly converting Fe-doped metal–organic frameworks into highly active and stable Fe-N-C catalysts for oxygen reduction in acid. Nano Energy, 2016, 25, 110-119.	8.2	434
3	MOF derived catalysts for electrochemical oxygen reduction. Journal of Materials Chemistry A, 2014, 2, 14064-14070.	5.2	407
4	Nanotechnology in Mg-based materials for hydrogen storage. Nano Energy, 2012, 1, 590-601.	8.2	250
5	A highly efficient and stable biphasic nanocrystalline Ni–Mo–N catalyst for hydrogen evolution in both acidic and alkaline electrolytes. Nano Energy, 2016, 22, 111-119.	8.2	166
6	Plasmaâ€Assisted Approaches in Inorganic Nanostructure Fabrication. Advanced Materials, 2010, 22, 1451-1473.	11.1	158
7	MOF-Derived Noble Metal Free Catalysts for Electrochemical Water Splitting. ACS Applied Materials & Interfaces, 2016, 8, 35390-35397.	4.0	151
8	MOF-derived surface modified Ni nanoparticles as an efficient catalyst for the hydrogen evolution reaction. Journal of Materials Chemistry A, 2015, 3, 16435-16439.	5.2	146
9	Air Plasma Activation of Catalytic Sites in a Metal yanide Framework for Efficient Oxygen Evolution Reaction. Advanced Energy Materials, 2018, 8, 1800085.	10.2	132
10	The impact of the particle size of a metal–organic framework for sulfur storage in Li–S batteries. Journal of Materials Chemistry A, 2015, 3, 8272-8275.	5.2	129
11	Ni–Mo Nanocatalysts on N-Doped Graphite Nanotubes for Highly Efficient Electrochemical Hydrogen Evolution in Acid. ACS Nano, 2016, 10, 10397-10403.	7.3	125
12	A Universal Method to Engineer Metal Oxide–Metal–Carbon Interface for Highly Efficient Oxygen Reduction. ACS Nano, 2018, 12, 3042-3051.	7.3	125
13	Photocatalytic Formaldehyde Oxidation over Plasmonic Au/TiO ₂ under Visible Light: Moisture Indispensability and Light Enhancement. ACS Catalysis, 2017, 7, 6514-6524.	5.5	121
14	Hydrogen storage properties of magnesium ultrafine particles prepared by hydrogen plasma-metal reaction. Materials Science and Engineering B: Solid-State Materials for Advanced Technology, 2004, 110, 221-226.	1.7	113
15	Polyoxometallates trapped in a zeolitic imidazolate framework leading to high uptake and selectivity of bioactive molecules. Journal of Materials Chemistry A, 2014, 2, 2168-2173.	5.2	102
16	Nickel-substituted zeolitic imidazolate frameworks for time-resolved alcohol sensing and photocatalysis under visible light. Journal of Materials Chemistry A, 2014, 2, 5724-5729.	5.2	98
17	Scalable graphene production: perspectives and challenges of plasma applications. Nanoscale, 2016, 8, 10511-10527.	2.8	97
18	A Peapodâ€like CoP@C Nanostructure from Phosphorization in a Lowâ€Temperature Molten Salt for Highâ€Performance Lithiumâ€Ion Batteries. Angewandte Chemie - International Edition, 2018, 57, 10187-10191.	7.2	87

#	Article	IF	CITATIONS
19	Perspectives and challenges of hydrogen storage in solid-state hydrides. Chinese Journal of Chemical Engineering, 2021, 29, 1-12.	1.7	87
20	Formation of Multiple-Phase Catalysts for the Hydrogen Storage of Mg Nanoparticles by Adding Flowerlike NiS. ACS Applied Materials & Interfaces, 2017, 9, 5937-5946.	4.0	84
21	A highly efficient Ni–Mo bimetallic hydrogen evolution catalyst derived from a molybdate incorporated Ni-MOF. Journal of Materials Chemistry A, 2018, 6, 9228-9235.	5.2	83
22	Alkali and Alkaline Earth Hydrides-Driven N ₂ Activation and Transformation over Mn Nitride Catalyst. Journal of the American Chemical Society, 2018, 140, 14799-14806.	6.6	81
23	MgCl 2 promoted hydrolysis of MgH 2 nanoparticles for highly efficient H 2 generation. Nano Energy, 2014, 10, 337-343.	8.2	78
24	Silica-Derived Hydrophobic Colloidal Nano-Si for Lithium-Ion Batteries. ACS Nano, 2017, 11, 6065-6073.	7.3	77
25	Noble Metal-Free Oxygen Reduction Reaction Catalysts Derived from Prussian Blue Nanocrystals Dispersed in Polyaniline. ACS Applied Materials & Interfaces, 2016, 8, 8436-8444.	4.0	76
26	Ultrafine Sn nanocrystals in a hierarchically porous N-doped carbon for lithium ion batteries. Nano Research, 2017, 10, 1950-1958.	5.8	76
27	An efficient Co–N–C oxygen reduction catalyst with highly dispersed Co sites derived from a ZnCo bimetallic zeolitic imidazolate framework. RSC Advances, 2016, 6, 37965-37973.	1.7	72
28	New approaches for rare earth-magnesium based hydrogen storage alloys. Progress in Natural Science: Materials International, 2017, 27, 50-57.	1.8	66
29	Enhancing the reactivity of nickel(<scp>ii</scp>) in hydrogen evolution reactions (HERs) by β-hydrogenation of porphyrinoid ligands. Chemical Science, 2017, 8, 5953-5961.	3.7	64
30	Lowâ€Temperature Synthesis of Honeycomb CuP ₂ @C in Molten ZnCl ₂ Salt for Highâ€Performance Lithium Ion Batteries. Angewandte Chemie - International Edition, 2020, 59, 1975-1979.	7.2	62
31	Tandem plasma reactions for Sn/C composites with tunable structure and high reversible lithium storage capacity. Nano Energy, 2013, 2, 1314-1321.	8.2	58
32	Improved Magnetic Anisotropy of Monodispersed Triangular Nickel Nanoplates. Journal of Physical Chemistry C, 2007, 111, 6630-6633.	1.5	54
33	The progress on aluminum-based anode materials for lithium-ion batteries. Journal of Materials Chemistry A, 2020, 8, 25649-25662.	5.2	53
34	Synthesis of Mg@Mg17Al12 ultrafine particles with superior hydrogen storage properties by hydrogen plasma–metal reaction. Journal of Materials Chemistry, 2012, 22, 19831.	6.7	52
35	A rare earth hydride supported ruthenium catalyst for the hydrogenation of <i>N</i> -heterocycles: boosting the activity <i>via</i> a new hydrogen transfer path and controlling the stereoselectivity. Chemical Science, 2019, 10, 10459-10465.	3.7	51
36	Highly efficient visible/near-IR-light-driven photocatalytic H2 production over asymmetric phthalocyanine-sensitized TiO2. RSC Advances, 2013, 3, 14363.	1.7	50

#	Article	IF	CITATIONS
37	Plasma Transforming Ni(OH) ₂ Nanosheets into Porous Nickel Nitride Sheets for Alkaline Hydrogen Evolution. ACS Applied Materials & Interfaces, 2020, 12, 5951-5957.	4.0	48
38	LaNi5.5 particles for reversible hydrogen storage in N-ethylcarbazole. Nano Energy, 2021, 80, 105476.	8.2	46
39	Direct plasma phosphorization of Cu foam for Li ion batteries. Journal of Materials Chemistry A, 2020, 8, 16920-16925.	5.2	44
40	Direct plasma deposition of amorphous Si/C nanocomposites as high performance anodes for lithium ion batteries. Journal of Materials Chemistry A, 2015, 3, 3522-3528.	5.2	40
41	Aluminum: An underappreciated anode material for lithium-ion batteries. Energy Storage Materials, 2020, 25, 93-99.	9.5	40
42	Hydrogen absorption–desorption, optical transmission properties and annealing effect of Mg thin films prepared by magnetron sputtering. International Journal of Hydrogen Energy, 2009, 34, 1910-1915.	3.8	39
43	Ultrafine Sn4P3 nanocrystals from chloride reduction on mechanically activated Na surface for sodium/lithium ion batteries. Nano Research, 2020, 13, 3157-3164.	5.8	39
44	The cutting-edge phosphorus-rich metal phosphides for energy storage and conversion. Nano Today, 2021, 40, 101245.	6.2	39
45	A Peapodâ€like CoP@C Nanostructure from Phosphorization in a Lowâ€Temperature Molten Salt for Highâ€Performance Lithiumâ€lon Batteries. Angewandte Chemie, 2018, 130, 10344-10348.	1.6	38
46	Ammonia borane confined by nitrogen-containing carbon nanotubes: enhanced dehydrogenation properties originating from synergetic catalysis and nanoconfinement. Journal of Materials Chemistry A, 2015, 3, 20494-20499.	5.2	34
47	Photosensitized Electron Injection from an ITO Electrode to Trichromophore Dyes Deposited on Langmuirâ^'Blodgett Films. Langmuir, 1999, 15, 7276-7281.	1.6	32
48	Promoting hydrogen absorption of liquid organic hydrogen carriers by solid metal hydrides. Journal of Materials Chemistry A, 2019, 7, 16677-16684.	5.2	32
49	Plasma modification of a Ni based metal–organic framework for efficient hydrogen evolution. Journal of Materials Chemistry A, 2019, 7, 8129-8135.	5.2	32
50	Hydrogen storage performances, kinetics and microstructure of Ti1.02Cr1.0Fe0.7-xMn0.3Alx alloy by Al substituting for Fe. Renewable Energy, 2020, 153, 1140-1154.	4.3	31
51	Chemical induced fragmentation of MOFs for highly efficient Ni-based hydrogen evolution catalysts. Nanoscale Horizons, 2018, 3, 218-225.	4.1	30
52	Interfacial Covalent Bonding Endowing Ti ₃ C ₂ ‣b ₂ S ₃ Composites High Sodium Storage Performance. Small, 2022, 18, e2104293.	5.2	30
53	Development of Ti1.02Cr2-x-yFexMny (0.6â‰ ¤ â‰ 9 .75, y=0.25, 0.3) alloys for high hydrogen pressure metal hydride system. International Journal of Hydrogen Energy, 2019, 44, 15087-15099.	3.8	28
54	Sn-C binary nanocomposites for lithium ion batteries: Core-shell vs. multilayer structure. Electrochimica Acta, 2018, 267, 1-7.	2.6	27

#	Article	IF	CITATIONS
55	SnSO4 modified ZnO nanostructure for highly sensitive and selective formaldehyde detection. Sensors and Actuators B: Chemical, 2018, 255, 1153-1159.	4.0	27
56	Novel Multifunctional Umbrella Molecule Material Combining Photoelectric Conversion and Second-Order Optical Nonlinearities in Langmuirâ´Blodgett Monolayers. Journal of Physical Chemistry B, 2000, 104, 5090-5095.	1.2	26
57	Excellent hydrogen sorption kinetics of thick Mg–Pd films under mild conditions by tailoring their structures. RSC Advances, 2013, 3, 4167.	1.7	26
58	Enhancement of Second Harmonic Generation and Photocurrent Generation of a Novel Stilbazolium Dye Dimer in Langmuirâ^'Blodgett Monolayer Films. Chemistry of Materials, 2001, 13, 192-196.	3.2	25
59	A miniature room temperature formaldehyde sensor with high sensitivity and selectivity using CdSO ₄ modified ZnO nanoparticles. RSC Advances, 2015, 5, 75098-75104.	1.7	25
60	Hydrogen storage properties of Y-Mg-Cu-H nanocomposite obtained by hydrogen-induced decomposition of YMg 4 Cu intermetallic. Journal of Alloys and Compounds, 2018, 751, 176-182.	2.8	25
61	Synergism of Rare Earth Trihydrides and Graphite in Lithium Storage: Evidence of Hydrogenâ€Enhanced Lithiation. Advanced Materials, 2018, 30, 1704353.	11.1	25
62	Improved hydrogen storage properties in Mg-based thin films by tailoring structures. International Journal of Hydrogen Energy, 2010, 35, 8331-8336.	3.8	24
63	Metal (metal = Fe, Co), N codoped nanoporous carbon for efficient electrochemical oxygen reduction. RSC Advances, 2014, 4, 37779-37785.	1.7	24
64	Mimicking of Tunichlorin: Deciphering the Importance of a β-Hydroxyl Substituent on Boosting the Hydrogen Evolution Reaction. ACS Catalysis, 2020, 10, 2177-2188.	5.5	24
65	Hydrogen desorption properties of Mg thin films at room temperature. Journal of Power Sources, 2010, 195, 1190-1194.	4.0	23
66	Lowâ€Temperature Synthesis of Honeycomb CuP ₂ @C in Molten ZnCl ₂ Salt for Highâ€Performance Lithium Ion Batteries. Angewandte Chemie, 2020, 132, 1991-1995.	1.6	23
67	Two pillared-layer metal–organic frameworks constructed with Co(ii), 1,2,4,5-benzenetetracarboxylate, and 4,4′-bipyridine: syntheses, crystal structures, and gas adsorption properties. CrystEngComm, 2012, 14, 2296.	1.3	22
68	Application of hydrogen for rare-earth gadolinium purification and thermodynamic simulation of system. Journal of Materials Science, 2019, 54, 13334-13343.	1.7	22
69	Interfacial covalent bonding enables transition metal phosphide superior lithium storage performance. Applied Surface Science, 2022, 582, 152404.	3.1	22
70	Weak ferromagnetism and spin-glass state with nanosized nickel carbide. Journal of Applied Physics, 2009, 105, 123923.	1.1	21
71	Superior hydrogen desorption kinetics of Mg(NH2)2 hollow nanospheres mixed with MgH2 nanoparticles. Applied Physics Letters, 2008, 92, 231910.	1.5	20
72	Room temperature solvent-free reduction of SiCl4 to nano-Si for high-performance Li-ion batteries. Chemical Communications, 2017, 53, 6223-6226.	2.2	20

#	Article	IF	CITATIONS
73	High-Performance Hydrogen Storage Nanoparticles Inside Hierarchical Porous Carbon Nanofibers with Stable Cycling. ACS Applied Materials & Interfaces, 2017, 9, 15502-15509.	4.0	20
74	Plasma enabled non-thermal phosphorization for nickel phosphide hydrogen evolution catalysts. Chemical Communications, 2019, 55, 4202-4205.	2.2	20
75	A monolithic sponge catalyst for hydrogen generation from sodium borohydride solution for portable fuel cells. Inorganic Chemistry Frontiers, 2021, 8, 35-40.	3.0	20
76	Experimental investigation and thermodynamic assessment of the yttrium-hydrogen binary system. Progress in Natural Science: Materials International, 2018, 28, 332-336.	1.8	19
77	Behavior of impurity elements in pure gadolinium during ultra-high purification. Vacuum, 2019, 162, 67-71.	1.6	19
78	Opposite particle size effects on the adsorption kinetics of ZIF-8 for gaseous and solution adsorbates. RSC Advances, 2015, 5, 58595-58599.	1.7	17
79	Highâ€pressure hydrogen storage properties of Ti x Cr 1 â~' y Fe y Mn 1.0 alloys. International Journal of Energy Research, 2019, 43, 5759-5774.	2.2	17
80	Efficient Synthesis of an Aluminum Amidoborane Ammoniate. Energies, 2015, 8, 9107-9116.	1.6	16
81	Promoted hydrogen release from alkali metal borohydrides in ionic liquids. Inorganic Chemistry Frontiers, 2016, 3, 1137-1145.	3.0	15
82	Synergism induced exceptional capacity and complete reversibility in Mg–Y thin films: enabling next generation metal hydride electrodes. Energy and Environmental Science, 2018, 11, 1563-1570.	15.6	15
83	Direct conversion of metal organic frameworks into ultrafine phosphide nanocomposites in multicomponent plasma for wide pH hydrogen evolution. Journal of Materials Chemistry A, 2020, 8, 10402-10408.	5.2	15
84	Combining catalysis and hydrogen storage in direct borohydride fuel cells: towards more efficient energy utilization. Journal of Materials Chemistry A, 2017, 5, 14310-14318.	5.2	14
85	Ni doping significantly improves dielectric properties of La2O3 films. Journal of Alloys and Compounds, 2020, 822, 153469.	2.8	13
86	Metal hydride mediated water splitting: Electrical energy saving and decoupled H2/O2 generation. Materials Today, 2021, 47, 16-24.	8.3	13
87	Removal of gaseous impurities from terbium byÂhydrogen plasma arc melting. International Journal of Hydrogen Energy, 2015, 40, 7943-7948.	3.8	12
88	Study on the thermodynamics of the gadolinium-hydrogen binary system (H/GdÂ=Â0.0–2.0) and implications to metallic gadolinium purification. Journal of Alloys and Compounds, 2016, 673, 131-137.	2.8	12
89	Hydrolysis Batteries: Generating Electrical Energy during Hydrogen Absorption. Angewandte Chemie - International Edition, 2018, 57, 2219-2223.	7.2	12
90	Plasma modified BiOCl/sulfonated graphene microspheres as efficient photo-compensated electrocatalysts for the oxygen evolution reaction. Catalysis Science and Technology, 2020, 10, 4786-4793.	2.1	12

#	Article	IF	CITATIONS
91	Hydrogen Generation by Hydrolysis of MgH2-LiH Composite. Materials, 2022, 15, 1593.	1.3	12
92	Experimental study and thermodynamic assessment of the dysprosium-hydrogen binary system. Journal of Alloys and Compounds, 2017, 696, 60-66.	2.8	11
93	Structure changes and optical properties of Mg2Ni switchable mirrors. International Journal of Hydrogen Energy, 2008, 33, 7207-7213.	3.8	10
94	Preparation and study of alkyl carbamylated polyrotaxanes with large hysteresis during sol–gel phase transition. Polymer Chemistry, 2011, 2, 1797.	1.9	10
95	Boric acid-destabilized lithium borohydride with a 5.6 wt% dehydrogenation capacity at moderate temperatures. Dalton Transactions, 2017, 46, 4499-4503.	1.6	10
96	Film formation from plasma-enabled surface-catalyzed dehalogenative coupling of a small organic molecule. RSC Advances, 2019, 9, 2848-2856.	1.7	10
97	A review of rare-earth oxide films as high k dielectrics in MOS devices— CommemoratingÂtheÂ100thÂanniversaryÂofÂtheÂbirthÂofÂAcademicianÂGuangxianÂXu. Journal of Rare Earths, 2021, 39, 121-128.	2.5	10
98	Synthesis and Hydrogen Storage Behaviour of Pure Mg ₂ FeH ₆ at Nanoscale. Materials Transactions, 2011, 52, 618-622.	0.4	9
99	Catalytic Thermal Decomposition of Ammonia–Borane by Wellâ€Dispersed Metal Nanoparticles on Mesoporous Substrates Prepared by Magnetron Sputtering. European Journal of Inorganic Chemistry, 2012, 2012, 5722-5728.	1.0	9
100	Effect of ammoniaâ€derived species on visibleâ€light photocatalytic activity of Au supported on amorphous TiO ₂ activated by plasma. Plasma Processes and Polymers, 2018, 15, 1800095.	1.6	9
101	Plasma-processed homogeneous magnesium hydride/carbon nanocomposites for highly stable lithium storage. Nano Research, 2018, 11, 2724-2732.	5.8	8
102	A high capacity nanocrystalline Sn anode for lithium ion batteries from hydrogenation induced phase segregation of bulk YSn ₂ . Journal of Materials Chemistry A, 2018, 6, 21266-21273.	5.2	8
103	Effect of heteroatoms on photocurrent generation from a series of styryl dye Langmuir–Blodgett films. Journal of Materials Chemistry, 2000, 10, 921-926.	6.7	7
104	Photoelectric conversion and second-order optical nonlinearity of Langmuir–Blodgett films of a novel dipolar two-dimensional material. Journal of Materials Chemistry, 2000, 10, 1287-1290.	6.7	7
105	Catalytic effect of (Ti _{0.85} Zr _{0.15}) _{1.05} Mn _{1.2} Cr _{0.6} V _{0.1hydrogen storage properties of ultrafine magnesium particles. RSC Advances, 2017, 7, 34538-34547.}	> ©a	071or
106	Stable, Efficient, Copper Coordination Polymer-Derived Heterostructured Catalyst for Oxygen Evolution under pH-Universal Conditions. ACS Applied Materials & Interfaces, 2021, 13, 25461-25471.	4.0	7
107	Mg2Si promoted magnesio-mechanical reduction of silica into silicon nanoparticles for high-performance Li-ion batteries. Journal of Solid State Chemistry, 2021, 302, 122408.	1.4	7
108	Arc-discharge synthesis of dual-carbonaceous-layer-coated tin nanoparticles with tunable structures and high reversible lithium storage capacity. Journal of Materials Chemistry A, 2017, 5, 13769-13775.	5.2	7

#	Article	IF	CITATIONS
109	Hydrogen generation from reactions of hydrides with hydrated solids in the solid state. RSC Advances, 2016, 6, 36863-36869.	1.7	5
110	The subtle role of heteroaromatics in the second-order susceptibility in a series of amphiphilic styryl dye Langmuir–Blodgett films. New Journal of Chemistry, 2000, 24, 317-321.	1.4	4
111	PREPARATION OF ZnO NANOPARTICLES BY PRECIPITATION/MECHANOCHEMICAL METHOD. International Journal of Nanoscience, 2002, 01, 563-567.	0.4	4
112	Yttrium trihydride enhanced lithium storage in carbon materials. Carbon, 2020, 164, 317-323.	5.4	4
113	Thermal stability and magnetic anisotropy of nickel nanoplates. Journal of Materials Science, 2009, 44, 4599-4603.	1.7	3
114	2-Aminoimidazole borohydride as a hydrogen carrier. RSC Advances, 2016, 6, 103299-103303.	1.7	3
115	Oxalic Acid Promoted Hydrolysis of Sodium Borohydride for Transition Metal Free Hydrogen Generation. Journal Wuhan University of Technology, Materials Science Edition, 2020, 35, 1011-1015.	0.4	3
116	Formation of polyhedral ceria nanoparticles with enhanced catalytic CO oxidation activity in thermal plasma via a hydrogen mediated shape control mechanism. Journal of Nanoparticle Research, 2011, 13, 4445-4450.	0.8	2
117	Hydrolysis Batteries: Generating Electrical Energy during Hydrogen Absorption. Angewandte Chemie, 2018, 130, 2241-2245.	1.6	2
118	Turning optical switching properties of Mg-Y films in electrochemical process by tailoring composition. Materials Research Express, 2018, 5, 036419.	0.8	1
119	Synthesis and dehydrogenation properties of NaZn(BH4)3Â∙en and NaZn(BH4)3•2en (en = ethylene diamin Journal of Energy Chemistry, 2020, 42, 233-236.	e) _{7.1}	1
120	Rücktitelbild: Hydrolysis Batteries: Generating Electrical Energy during Hydrogen Absorption (Angew.) Tj ETQq0	0.0 rgBT 1.6	/Overlock 10

121	Oxalic Acid Promoted Hydrolysis of Sodium Borohydride for Transition Metal Free Hydrogen Generation. Journal Wuhan University of Technology, Materials Science Edition, 2020, 35, 706-710.	0.4	0
122	lonization inhibition in a polyol/water system for boosting H ₂ generation from NaBH ₄ . RSC Advances, 2021, 11, 510-516.	1.7	0
123	PREPARATION OF ZnO NANOPARTICLES BY PRECIPITATION/MECHANOCHEMICAL METHOD., 2003, , .		0